

Ultrafast Infrared Mechanistic Studies of the Interaction of 1-Hexyne with Group 6 Hexacarbonyl Complexes

Jennifer E. Shanoski, Christine K. Payne, Matthias F. Kling,
Elizabeth A. Glascoe, and Charles B. Harris*

Department of Chemistry, University of California, Berkeley, California 94720, and Chemical Sciences Division, Lawrence Berkeley National Laboratory, Berkeley, California 94720

Received November 19, 2004

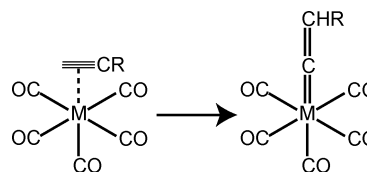
The ultrafast solvation and rearrangement dynamics following the photolysis of $M(\text{CO})_6$ ($M = \text{Cr}, \text{Mo}, \text{W}$) in terminal alkyne solutions have been investigated. Upon photoinitiated loss of a ligand from the parent metal hexacarbonyl, coordination to an alkyne solvent molecule is followed by rearrangement to a complex that is bound to the terminal alkyne site in a π -bonded fashion. This rearrangement occurs on a time scale that is anticorrelated with the metal–ligand binding energy. A dissociative rearrangement is ruled out for this process in favor of an associative or interchange mechanism. Previous theoretical and experimental studies are examined, and we conclude that the ultimate rearrangement to a vinylidene species is energetically inaccessible at ambient temperatures on the femtosecond to millisecond time scale.

I. Introduction

The coordination of unsaturated hydrocarbons to transition metal complexes is important for both fundamental and industrial applications due to the essential role these complexes play in the synthesis of hydrocarbon products.¹ Examples of such reactions include polymerization, metathesis, and cyclo-oligomerization.^{2–4} Knowledge of the mechanistic details of this coordination is the key to controlling such reactions, providing the possibility of selective functionalization. Many of the reactions involving the complexation of unsaturated hydrocarbons to transition metal centers are thought to proceed via the formation of a vinylidene metal species. Particular interest has centered on the photoinduced coordination and rearrangement of transition metal carbonyl complexes, such as $M(\text{CO})_6$ ($M = \text{W}, \text{Cr}, \text{Mo}$) with terminal alkynes.^{5–7}

Upon photodissociation of a single carbonyl from a parent metal hexacarbonyl complex, the first step in many condensed phase reactions is the interaction of the unsaturated metal center with a neighboring solvent molecule.^{8,9} In terminal alkyne solutions, this solvation is thought to yield a π -bond coordinated complex which rearranges to the vinylidene species as shown in Scheme 1. Previous ultrafast studies on group 6 metal hexacarbonyl complexes in alcohol and silane solutions, however, revealed that solvation is more complex and

Scheme 1. Schematic Representation of the Tautomerization from the π -Bonded Alkyne Complex to the Vinylidene-Metal Complex



may involve initial coordination at any site of the functionalized solvent molecule with subsequent rearrangement to a more stable configuration.¹⁰ Although considerable interest has focused on the coordination and rearrangement of transition metal complexes with terminal alkynes, a clear consensus on the mechanistic details of the reaction has not yet been reached. The original mechanism proposed for the photoinduced reaction of metal carbonyl complexes with terminal alkynes is based on low-temperature matrix studies.^{11–13} These experiments provided information about possible intermediates formed in the photoinduced reaction, but because these experiments were conducted at low temperatures in glassy matrixes, solvent effects were not explicitly studied and the initial coordination steps could not be investigated.

Experimental and theoretical results obtained in other work suggest that the formation of a vinylidene species is highly dependent on the particular system studied. Experimental ESR measurements have focused on the rearrangement of $[\text{Cr}(\text{CO})_2(\eta^2\text{-Me}_3\text{-SiC}\equiv\text{CSiMe}_3)(\eta\text{-$

* To whom correspondence should be addressed. E-mail: harris@socrates.berkeley.edu.

- (1) Bruneau, C.; Dixneuf, P. H. *Acc. Chem. Res.* **1999**, *32*, 311.
- (2) Gita, B.; Sundararajan, G. *Tetrahedron Lett.* **1993**, *34*, 6123.
- (3) Duplessis, J. A. K.; Vosloo, H. C. M. *J. Mol. Catal.* **1991**, *65*, 51.
- (4) Landon, S. J.; Shulman, P. M.; Geoffroy, G. L. *J. Am. Chem. Soc.* **1985**, *107*, 6739.
- (5) Szymanska-Buzar, T. *J. Mol. Catal.* **1988**, *48*, 43.
- (6) Szymanska-Buzar, T. *J. Mol. Catal.* **1994**, *93*, 137.
- (7) Bruce, M. I. *Chem. Rev.* **1991**, *91*, 197, and references therein.
- (8) Simon, J. D.; Xie, X. L. *J. Phys. Chem.* **1986**, *90*, 6751.
- (9) Simon, J. D.; Xie, X. L. *J. Phys. Chem.* **1987**, *91*, 5538.

(10) Kotz, K. T.; Yang, H.; Snee, P. T.; Payne, C. K.; Harris, C. B. *J. Organomet. Chem.* **2000**, *596*, 183.

(11) Szymanska-Buzar, T.; Kern, K. *J. Organomet. Chem.* **2001**, *622*, 74.

(12) Szymanska-Buzar, T.; Downs, A. J.; Greene, T. M.; Marshall, A. S. *J. Organomet. Chem.* **1995**, *495*, 149.

(13) Szymanska-Buzar, T.; Downs, A. J.; Greene, T. M.; Marshall, A. S. *J. Organomet. Chem.* **1995**, *495*, 163.

C_6Me_6] to its vinylidene analogue.¹⁴ The rate constant was measured to be $k = 0.31 \text{ s}^{-1}$ at room temperature, indicating a high barrier for the thermal reaction. Other recent work on metal–carbonyl complexes $M(CO)_5-HC\equiv CR$ ($M = Cr, Mo, W$) utilizing steady-state infrared and NMR spectroscopic techniques suggests an equilibrium between the π -bonded complex and the corresponding vinylidene species, while the former is thought to be thermodynamically favored.¹⁵ The vinylidene complex could only be isolated with trapping methods in this case. In contrast, DFT calculations carried out by De Angelis and co-workers on $Cp(PMe_3)_2Ru(HC\equiv CR)$ suggest that the vinylidene species is energetically favored over the π -bonded complex by 13.1 kcal/mol.¹⁶

The group 6 metal carbonyl complexes, $M(CO)_5-HC\equiv CR$ ($M = Cr, Mo, W$; $R = C_4H_7$), studied in this work are expected to undergo a similar type of tautomerization¹⁷ from a π -bonded complex to a vinylidene metal complex. Interestingly, the formation of the vinylidene species in the photochemistry of $M(CO)_6$ complexes in terminal alkynes has been attributed to both thermal effects¹⁸ and/or sequential photoexcitation.^{12,13} In light of these ambiguities, a femtosecond infrared study of the photoinitiated reaction of $M(CO)_6$ ($M = Cr, W, Mo$) in neat alkyne solutions was carried out in order to clarify the mechanism. This technique can follow reaction dynamics on the time scales (femtoseconds to nanoseconds) over which they occur in ambient solutions.¹⁹ Such a method is particularly well-suited to the investigation of transition metal–carbonyl complexes because the carbonyl stretching frequencies are highly sensitive to changes in the electron density at the metal center.

In addition to expanding the understanding of the mechanism of vinylidene formation, the current experiments aim to extend the understanding of rearrangement for metal–carbonyl complexes in coordinative solvents. All previous experiments have focused on the rearrangement of the π -bonded complex to the vinylidene complex without any consideration of the initial solvation. The primary steps of coordination and rearrangement are not yet understood and should provide important mechanistic details of the process. To the best of our knowledge, no study has yet been carried out on the solvation and rearrangement dynamics of transition metal carbonyls in unsaturated hydrocarbon solutions.²⁰

This work details the early time dynamical behavior of group 6 metal hexacarbonyl complexes in terminal

alkyne solutions. The initial solvation and rearrangement steps are followed for 1-hexyne and compared with previous studies of functionalized hydrocarbon solutions.¹⁰ The mechanism of the rearrangement process is analyzed in the context of the binding energy of the metal fragment to the solvent ligand. Additionally, the possibility of vinylidene formation is investigated on the femtosecond to millisecond time scales.

II. Methods

A. Experimental Apparatus. The experimental apparatus consists of a Ti:sapphire regenerative amplifier (SpectraPhysics, Spitfire) seeded by a Ti:sapphire oscillator (SpectraPhysics, Tsunami) to produce a 1 kHz pulse train of 100 fs pulses centered at 800 nm with an average pulse power of 0.9 mJ. The output of this system is split and used for both harmonic generation of 266 nm pump pulses and to pump a home-built optical parametric amplifier (OPA) to deliver tunable mid-IR probe pulses (3.0–6.0 μm). A computer-controlled translation stage (Klinger) allows for variable time delays between pump and probe pulses.

The OPA used in this setup is based on that described by Hamm and co-workers.²¹ Infrared pulses tunable from 3 to 6.0 μm with a spectral width of ca. 200 cm^{-1} and pulse durations around 100 fs are routinely generated. The IR probe beam is split after the OPA into signal and reference lines using a 50% germanium beam splitter. The signal line is focused using a CaF_2 lens to provide a beam diameter at the sample of 100 μm . The pump beam is focused using a CaF_2 lens to a diameter of 200 μm at the sample. The maximum power of generated 266 nm light is 4 μJ , but can be reduced to smaller powers when required by specific experimental considerations. The sample is flowed using a mechanical pump through a cell (Harrick Scientific) fitted with 1.5 mm thick MgF_2 windows. The optical path length in these experiments was 150 μm , and sample concentrations were adjusted so that the optical density (OD) of the sample at the pump wavelength was ~ 1 . The sample is moved perpendicular to the laser beam by computer-controlled translational stages (Standa) after each measured spectrum to ensure that absorptions are not masked or enhanced due to burning effects, which result in secondary product accumulation on the cell windows.

The pump and signal beams are overlapped in space and cross-correlated using a silica wafer to identify time zero. The pulse width is 100–150 fs. Reference and signal IR beams are sent through a computer-controlled spectrograph (Acton Research Corporation, SpectraPro-150) along a parallel path. The entrance slits on the spectrograph are routinely set at 35 μm to achieve a spectral resolution of $\sim 3 \text{ cm}^{-1}$. Spectrally dispersed signal and reference beams are detected by a 2×32 element MCT-array IR detector (InfraRed Associates, Inc.) and a high-speed signal acquisition system (Infrared Systems Development Corp.). In part of the experiments, reference and signal infrared beams were sent through a monochromator (CVI, Digikrom 240) with a spectral resolution of ca. $\pm 2 \text{ cm}^{-1}$ at a slit width of 400 μm and detected by single-element MCT IR-detectors (Electro-Optical Systems). Collected signals are typically normalized over 1000 laser shots to account for shot-to-shot fluctuations of the laser. Differences in optical density (ΔOD) as small as 5×10^{-5} can be observed in the experiments with 1 s of signal averaging.

B. Sample Handling. Metal hexacarbonyl complexes, $M(CO)_6$ ($M = Cr, Mo, W$), were purchased from Strem. Spectroscopic grade 1-hexyne was purchased from Sigma-Aldrich. All chemicals were used without further purification.

C. Computational Details. Density functional theory (DFT) calculations have been used in this work to assist in the characterization of the observed intermediate species. The results from DFT calculations described here were carried out

(14) Connelly, N. G.; Geiger, W. E.; Lagunas, M. C.; Metz, B.; Rieger, A. L.; Rieger, P. H.; Shaw, M. J. *J. Am. Chem. Soc.* **1995**, *117*, 12202.

(15) Abd-Elzaher, M. M.; Fischer, H. *J. Organomet. Chem.* **1999**, *588*, 235.

(16) De Angelis, F.; Sgamellotti, A.; Re, N. *Organometallics* **2002**, *21*, 5944.

(17) Tautomerization in this work refers to the rearrangement from a π -bonded complex to a vinylidene-metal complex. Cadierno, V.; Gamasa, M. P.; Gimeno, J.; Gonzalez-Bernardo, C.; Perez-Carreno, E.; Garcia-Granda, S. *Organometallics* **2001**, *20*, 5177.

(18) Birdwhistell, K. R.; Burgmayer, S. J. N.; Templeton, J. L. *J. Am. Chem. Soc.* **1983**, *105*, 7789.

(19) For example: Bromberg, S. E.; Yang, H.; Asplund, M. C.; Lian, T.; McNamara, B. K.; Kotz, K. T.; Yeston, J. S.; Wilkens, M.; Frei, H.; Bergman, R. G.; Harris, C. B. *Science* **1997**, *278*, 260.

(20) Studies have been carried out for group 6 metal hexacarbonyl complexes in n-hexane/n-hexene solutions, but did not address the fundamental solvation questions posed in this work. Dougherty, T. P.; Heilweil, E. J. *J. Chem. Phys.* **1994**, *100*, 4006.

(21) Hamm, P.; Kaindl, R. A.; Stenger, J. *Opt. Lett.* **2000**, *25*, 1798.

using Gaussian03,²² Becke's three-parameter exchange–correlation energy²³ combined with the Lee–Yang–Parr correlation functional,²⁴ B3LYP,²⁵ was used in all calculations. The basis set used for the main group elements consisted of the 6-311G** basis functions,^{26,27} and the LANL2DZ core potential²⁸ was used for all of the central transition metals.²⁹ Frequency calculations were carried out in order to ensure that configurations obtained correspond to minima or first-order saddle points on the potential energy surface and are used in the spectral analysis of the data. DFT calculations have been shown to be reliable in calculations of the type used here for transition metal complexes.^{30,31}

D. Data Analysis. Kinetic traces in this work are the result of changes in the peak intensities. The peaks are integrated and normalized according to the spectral width of the analyzed region. The data are fit to an instrument response function characterized by the temporal resolution of the experimental setup, 150 fs, and a single-exponential function. This is appropriate for all of the dynamics in this work since a single growth pathway exists for all species and no decay component is observed. A χ -squared fitting routine using the relative peak area and the associated error was used for all kinetic parameters reported in this work. Errors for kinetic fits are obtained using a Monte Carlo bootstrap method in which 1000 simulated data sets were used to estimate the errors. Errors here are reported as 95% confidence limits.

Spectral changes in the carbonyl stretching frequencies are recorded as difference spectra in which a spectrum collected at negative time delays (-15 ps) is subtracted from all spectra collected after photoinitiation. Spectra were fit according to the sum of Gaussian functions with a vertical offset parameter in order to carry out the peak width narrowing analysis described in the results. All fitting parameters were determined using a χ -squared minimization. The fitting of spectra was done iteratively where the optimized parameters of an early time slice were used as an initial guess for the parameters of the subsequent time slice.

III. Results and Discussion

A. Experimental Results and Mechanistic Explanation. Ultrafast UV-pump IR-probe experiments

(22) Frisch, M. J.; Trucks, G. W.; Schlegel, H. B.; Scuseria, G. E.; Robb, M. A.; Cheeseman, J. R.; Montgomery, J. A., Jr.; Vreven, T.; Kudin, K. N.; Burant, J. C.; Millam, J. M.; Iyengar, S. S.; Tomasi, J.; Barone, V.; Mennucci, B.; Cossi, M.; Scalmani, G.; Rega, N.; Petersson, G. A.; Nakatsuji, H.; Hada, M.; Ehara, M.; Toyota, K.; Fukuda, R.; Hasegawa, J.; Ishida, M.; Nakajima, T.; Honda, Y.; Kitao, O.; Nakai, H.; Klene, M.; Li, X.; Knox, J. E.; Hratchian, H. P.; Cross, J. B.; Adamo, C.; Jaramillo, J.; Gomperts, R.; Stratmann, R. E.; Yazyev, O.; Austin, A. J.; Cammi, R.; Pomelli, C.; Ochterski, J. W.; Ayala, P. Y.; Morokuma, K.; Voth, G. A.; Salvador, P.; Dannenberg, J. J.; Zakrzewski, V. G.; Dapprich, S.; Daniels, A. D.; Strain, M. C.; Farkas, O.; Malick, D. K.; Rabuck, A. D.; Raghavachari, K.; Foresman, J. B.; Ortiz, J. V.; Cui, Q.; Baboul, A. G.; Clifford, S.; Cioslowski, J.; Stefanov, B. B.; Liu, G.; Liashenko, A.; Piskorz, P.; Komaromi, I.; Martin, R. L.; Fox, D. J.; Keith, T.; Al-Laham, M. A.; Peng, C. Y.; Nanayakkara, A.; Challacombe, M.; Gill, P. M. W.; Johnson, B.; Chen, W.; Wong, M. W.; Gonzalez, C.; Pople, J. A. *Gaussian 03*; Gaussian, Inc.: Pittsburgh, PA, 2003.

(23) Becke, A. D. *J. Chem. Phys.* **1993**, *98*, 5648.

(24) Lee, C. T.; Yang, W. T.; Parr, R. G. *Phys. Rev. B* **1988**, *37*, 785.

(25) Stephens, P. J.; Devlin, F. J.; Chabalowski, C. F.; Frisch, M. J. *J. Phys. Chem.* **1994**, *98*, 11623.

(26) Hehre, W. J.; Ditchfield, R.; Pople, J. A. *J. Chem. Phys.* **1972**, *56*, 2257.

(27) Francl, M. M.; Pietro, W. J.; Hehre, W. J.; Binkley, J. S.; Gordon, M. S.; Defrees, D. J.; Pople, J. A. *J. Chem. Phys.* **1982**, *77*, 3654.

(28) Hay, P. J.; Wadt, W. R. *J. Chem. Phys.* **1985**, *82*, 299.

(29) 1-Propane and propane were used instead of 1-hexyne in our calculations to minimize the computational time. Such approximations have been shown to provide appropriate values for the relative energies, frequencies, and peak intensities of comparable complexes.

(30) Glukhovtsev, M. N.; Bach, R. D.; Nagel, C. J. *J. Phys. Chem. A* **1997**, *101*, 316.

(31) Ricca, A.; Bauschlicher, C. W. *Theor. Chim. Acta* **1995**, *92*, 123.

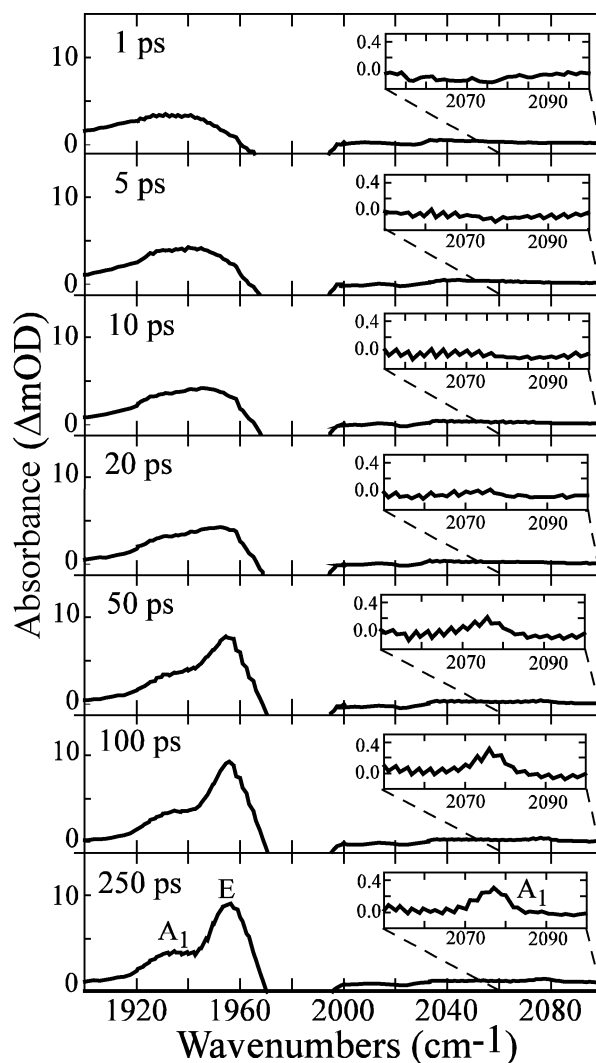


Figure 1. $\text{Cr}(\text{CO})_6$ in 1-hexyne at increasing delay times after photodissociation of a single carbonyl group. The broad peaks present at early times indicate the presence of a vibrationally excited, solvated product. As they vibrationally cool, these peaks eventually narrow and shift. At 250 ps three peaks are visible; at 1929 and 1960 cm^{-1} are the A_1 and E band of the initially solvated species, and at 2076 cm^{-1} the A_1 band of the π -bound species (**2**) is visible. Small oscillations in the data are the result of collecting two spectra offset by 1 cm^{-1} from each other and interleaving them together.

were carried out for each of the group 6 metal hexacarbonyls: $\text{Cr}(\text{CO})_6$, $\text{Mo}(\text{CO})_6$, and $\text{W}(\text{CO})_6$. The spectra obtained for a room-temperature solution of $\text{Cr}(\text{CO})_6$ in 1-hexyne at increasing delay times after photoexcitation are shown in Figure 1. All three metal hexacarbonyl species demonstrate the same behavior; spectra for $\text{Mo}(\text{CO})_6$ and $\text{W}(\text{CO})_6$ can be found in the Supporting Information. The parent bleach appears as a negative absorption, indicating the depletion of parent molecules, and the appearance of new species are indicated by positive absorptions. The relevant spectral features for all three complexes are given in Table 1.

The general behavior of metal hexacarbonyl complexes after UV photoexcitation has been extensively studied.^{32–36} Upon irradiation, a single carbonyl group

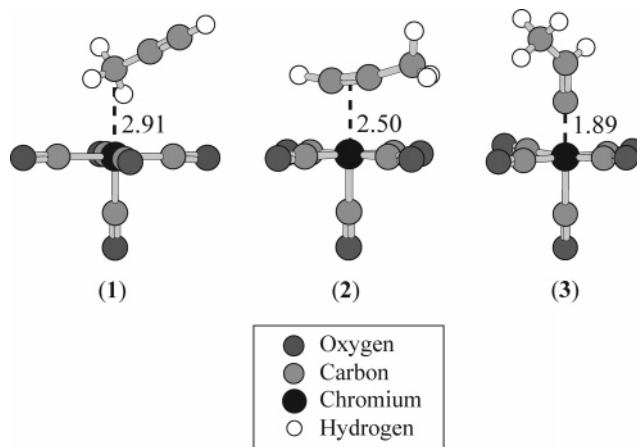
(32) Dougherty, T. P.; Heilweil, E. J. *Chem. Phys. Lett.* **1994**, *227*, 19.

Table 1. Peak Positions for Ultrafast Experiments (in wavenumbers (cm^{-1})) for All Three Metal Complexes: Cr, Mo, and W (errors are ca. $\pm 2 \text{ cm}^{-1}$)

peak assignment	Cr(CO) ₅ -L	Mo(CO) ₅ -L	W(CO) ₅ -L
A ₁	1929	1935	1933
E	1960	1962	1957
A ₁	2076	2085	2086

dissociates from the metal carbonyl complex within 100 fs.³³ Inspection of the time-resolved spectra for Cr(CO)₆ in neat 1-hexyne shows a parent bleach at 1987 cm^{-1} , indicating the depletion of parent species due to carbonyl loss. The bleach is cut out of the spectra in Figure 1 for better visualization. The appearance of broad peaks in the spectrum at the earliest delay time of 1 ps indicates the formation of a solvated complex in agreement with the solvation times for other metal carbonyl complexes in solution.^{8,9,34,36} Solvation here refers to the interaction of the metal center with a molecule from the bath without distinguishing the manner in which the complexation occurs. Since the amount of energy delivered to the parent molecule far exceeds that required to dissociate a single carbonyl group, the solvated complex is vibrationally excited. This excess energy is quickly distributed among the various modes of the complex and is transferred to the surrounding bath. This process of vibrational relaxation is well characterized^{32,36-43} and can be seen in the spectra for Cr(CO)₆ in neat 1-hexyne via the narrowing and shifting of the three peaks until they reach their equilibrium absorption frequencies of 1929, 1960, and 2076 cm^{-1} .

To provide assignments for the observed peaks, it is necessary to consider all possible outcomes of the initial solvation. 1-Hexyne has two effective bonding arrangements: in a σ -bonded fashion to one of the alkyl sites of the alkyl chain or in a π -bonded fashion to the triple bond of the alkyne. The DFT optimized geometries of the two possible solvated complexes as well as the vinylidene complex are shown in Figure 2. The three structures are labeled as **1**, the σ -bonded complex; **2**, the π -bonded complex; and **3**, the vinylidene complex, and will be referred to as such throughout the remainder of this paper. The calculated absorption frequencies⁴⁴ of complexes **1** and **2** are shown in Table 2 and agree well with the previous experimental trends shown in Table 3.^{12,13} Also in Table 2 are the calculated relative peak intensities for all of the absorption frequencies. The peaks at 1929 and 2076 cm^{-1} correspond

**Figure 2.** Optimized geometries of the σ -bonded intermediate (**1**), the π -bonded intermediate (**2**), and the vinylidene complex (**3**). All calculations were done using 1-propyne.²⁹ Bond lengths (in Å) are shown for the metal-alkyne interaction.**Table 2. Calculated Frequencies (in cm^{-1}) for Complexes 1 and 2 for All Three Metals: Cr, Mo, and W (normalized absorption intensities are given in parentheses)**

peak assignment	Cr(CO) ₅ -L	Mo(CO) ₅ -L	W(CO) ₅ -L	
1	A ₁	1965.7 (0.24)	1953.2 (0.24)	1950.2 (0.24)
	E	1982.4 (1.00)	1979.1 (1.00)	1969.4 (1.00)
2	A ₁	2078.9 (0.01)	2080.9 (0.01)	2078.8 (0.02)
	A ₁	1961.7 (0.28)	1955.5 (0.26)	1955.7 (0.22)
	E	1966.7 (1.00)	1964.9 (1.00)	1964.4 (1.00)
	A ₁	2064.2 (0.04)	2069.4 (0.03)	2072.3 (0.04)

Table 3. Experimental Carbonyl Absorption Frequencies from Previous Low-Temperature Matrix Studies (in wavenumbers (cm^{-1})) for Complexes 2 and 3 for Mo¹² and W^{13a}

peak assignment	Mo(CO) ₅ -L	W(CO) ₅ -L	
1	A ₁	1927 (m)	1926
	E	1930 (m)	
	E	1969 (vs)	1957.5
2	A ₁	1971 (vs)	
	A ₁	2092 (w)	2092
	A ₁	1945 (w)	1950 (w)
	E	1968 (vs)	1978 (m)
	E	1974 (s)	
3	A ₁	2088 (w)	2093 (w)
	E	2000 (w)	
	A ₁	2078 (w)	
		2074 (w)	

^a Complex **1** in this table is the methane coordinated complex from the same low-temperature studies in a methane matrix. Absorption intensities are shown in parentheses where available, with w = weak, m = medium, s = strong, and vs = very strong. Bands for which two frequencies are listed are the result of splitting by matrix side effects.

to two A₁ bands, and the peak at 1960 cm^{-1} corresponds to the E band of the solvated species with local C_{4v} symmetry.^{12,13} These assignments do not distinguish between the two possible solvated intermediates, but are general, as the local symmetry of both complexes is the same. The calculated absorption frequencies for all bands of **1** and **2** are very similar, and therefore the frequencies alone cannot be used to isolate the mechanistic details of this reaction. It is important, however, to note that the calculated absorption intensity of the A₁ band around 2080 cm^{-1} is 4 times as large for **2** than for **1** in the chromium complex.

(33) Lian, T. Q.; Bromberg, S. E.; Asplund, M. C.; Yang, H.; Harris, C. B. *J. Phys. Chem.* **1996**, *100*, 11994.

(34) Joly, A. G.; Nelson, K. A. *Chem. Phys.* **1991**, *152*, 69.

(35) Xie, X. L.; Simon, J. D. *J. Am. Chem. Soc.* **1990**, *112*, 1130.

(36) King, J. C.; Zhang, J. Z.; Schwartz, B. J.; Harris, C. B. *J. Chem. Phys.* **1993**, *99*, 7595.

(37) Dougherty, T. P.; Grubbs, W. T.; Heilweil, E. J. *J. Phys. Chem.* **1994**, *98*, 9396.

(38) George, M. W.; Dougherty, T. P.; Heilweil, E. J. *J. Phys. Chem.* **1996**, *100*, 201.

(39) Arrivo, S. M.; Dougherty, T. P.; Grubbs, W. T.; Heilweil, E. J. *Chem. Phys. Lett.* **1995**, *235*, 247.

(40) Heilweil, E. J.; Cavanagh, R. R.; Stephenson, J. C. *Chem. Phys. Lett.* **1987**, *134*, 181.

(41) Heilweil, E. J.; Cavanagh, R. R.; Stephenson, J. C. *J. Chem. Phys.* **1988**, *89*, 230.

(42) Iannone, M.; Cowen, B. R.; Diller, R.; Maiti, S.; Hochstrasser, R. M. *Appl. Opt.* **1991**, *30*, 5247.

(43) Tokmakoff, A.; Sauter, B.; Fayer, M. D. *J. Chem. Phys.* **1994**, *100*, 9035.

(44) All calculated frequencies have been scaled by a factor of 0.9614. Scott, A. P.; Radom, L. *J. Phys. Chem.* **1996**, *100*, 16502.

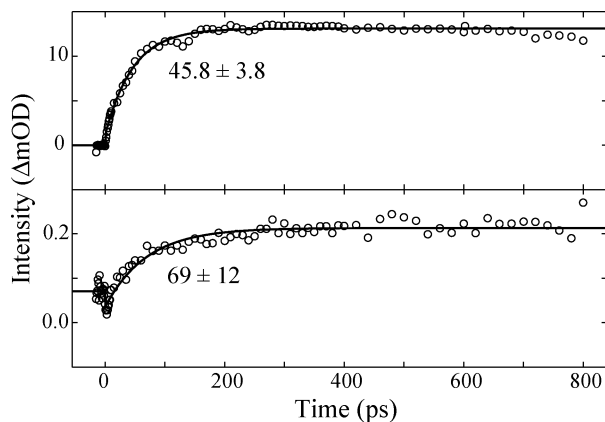


Figure 3. Kinetic traces for Cr(CO)₅ in 1-hexyne: (a) E band centered at 1960 cm⁻¹; (b) A₁ band centered at 2076 cm⁻¹. Open circles represent experimental data and lines represent fits to the data with time constants shown.

Table 4. Rise Time Constants (in ps) Obtained from Single-Exponential Fits of M(CO)₅ in 1-Hexyne Obtained for the E Band Centered around 1960 cm⁻¹ and the A₁ Band Centered around 2080 cm^{-1a}

	E band	A ₁ band
Cr(CO) ₅	45.8 ± 3.8	68 ± 12
Mo(CO) ₅	42.3 ± 3.2	86 ± 11
W(CO) ₅	28.0 ± 6.3	36 ± 6

^a Errors are 95% confidence limits.

Inspection of the kinetic traces for the transient absorptions provides additional relevant information. Shown in Figure 3 are kinetic traces for the E band centered at 1960 cm⁻¹ and A₁ band centered at 2076 cm⁻¹. A kinetic trace of the A₁ band centered at 1929 cm⁻¹ is not shown because the early time dynamics are obscured by the vibrationally hot population of E, as can be seen in the early time spectra shown in Figure 1. The traces show first-order kinetic behavior in all cases. The rise times for the chromium complex absorptions at 1960 and 2076 cm⁻¹ were found to be 45.8 ± 3.8 and 68 ± 12 ps, respectively. Table 4 summarizes the time constants that result from first-order kinetic fits for all three metal-carbonyl complexes. The significant difference between the time constants for the two peaks indicates that different kinetic processes are occurring.

The shorter time constant, 45.8 ± 3.8 ps, is a measure of the vibrational relaxation time of the E band of the initially solvated complex and contains information about both species **1** and **2** due to their strong overlap. To verify this statement, the vibrational relaxation time was estimated using the product band narrowing method.³⁷ A Gaussian function was chosen to fit the spectra in order to obtain peak width estimates. The variation of the peak width over time was fit according to the relationship

$$\Delta\nu_{\text{abs}}(t) = [(A \exp^{-t/\tau} + \Gamma)^2 + (\text{IRF})^2]^{1/2}$$

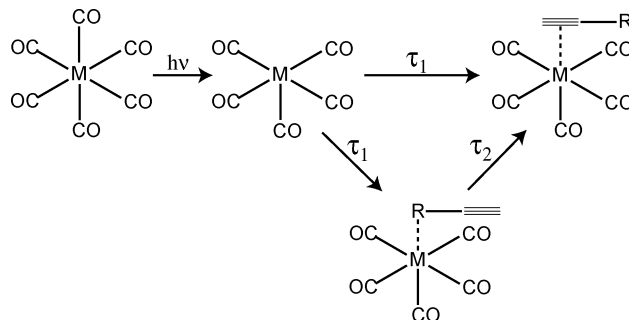
where Γ is the long-time width, A is the additional width, τ is the cooling time, and IRF is the spectral instrument response (2 cm⁻¹ here). Table 5 gives the fit parameters for all three metal carbonyl complexes according to an analysis of this type. The vibrational relaxation times agree well with the values obtained by

Table 5. Vibrational Relaxation Fitting Parameters for M(CO)₅ in 1-Hexyne^a

	A (cm ⁻¹)	τ (ps)	Γ (cm ⁻¹)
Cr(CO) ₅	3.0 ± 0.5	42.5 ± 6.6	6.0
Mo(CO) ₅	12.5 ± 3.5	32.5 ± 7.7	7.0
W(CO) ₅	7.0 ± 2.0	34.3 ± 9.1	9.8

^a The long time width (Γ) is fixed according to the spectra.

Scheme 2. Proposed Rearrangement Sequence for M(CO)₆ in 1-Hexyne^a



^a The initial coordination can be to any of the carbon sites on the alkyl chain of the alkyne in a σ -bonded fashion or to the triple bond in a π -bonded fashion.

fitting the rise time of the E band. The time scale for vibrational relaxation measured here also falls within the range of previously reported values of 5–50 ps.^{34,36}

We propose that the longer time constant, 68 ± 12 ps, measured for the A₁ band at 2076 cm⁻¹ is solely representative of complex **2**. The small peak does not shift or narrow as it increases in intensity, indicating that the time constant is not a measure of vibrational relaxation of the A₁ band. Instead, this long time constant represents the amount of time required for the rearrangement of complexes of type **1** to complex **2**. Previous work has demonstrated that a coordinated alkyl group can be best described as a “token ligand” which interacts weakly with the metal center.^{45–47} If a stronger interaction is possible, as there is in a terminal alkyne via the π -bond, then rearrangement to the thermodynamically favored product results. Thus, in 1-hexyne, any σ -bound complex **1** will eventually rearrange to the π -bound complex **2**. Scheme 2 shows the proposed rearrangement mechanism. The E band absorption is insensitive to the rearrangement because both **1** and **2** exhibit a large peak at this frequency; any decay in the absorption of **1** is concomitant with an increase in the absorption of **2**, resulting in no net absorbance change.

An important piece of information in assigning the longer time constant to the rearrangement is the relative intensities of the absorption of the A₁ band around 2080 cm⁻¹ (Table 2). These values indicate that although the absorption frequencies are very similar for **1** and **2**, the intensities of these absorptions differ. To identify which solvated product is responsible for the experimentally observed absorption, a comparison can be made between the experimental peak ratios and the calculated peak ratios for each of the possible solvated

(45) Periana, R. A.; Bergman, R. G. *J. Am. Chem. Soc.* **1986**, *108*, 7332.

(46) Dobson, G. R.; Hodges, P. M.; Healy, M. A.; Poliakoff, M.; Turner, J. J.; Firth, S.; Asahi, K. *J. Am. Chem. Soc.* **1987**, *109*, 4218.

(47) Hall, C.; Perutz, R. N. *Chem. Rev.* **1996**, *96*, 3125.

species. In the chromium experiments, the peaks at 1929, 1960, and 2076 cm^{-1} have calculated oscillator strength ratios of 24:100:1 for **1** and 28:100:4 for **2**. The experimental peak ratio at long time delays is 28:100:4, in excellent agreement with the calculated ratio for **2**. The use of relative absorption intensities has been extensively tested for transition metal complexes and has been verified to qualitatively reproduce experimental spectra.^{48–50}

To verify the absence of an absorption for **1** in the region around 2080 cm^{-1} , the experiment was repeated in neat hexane under otherwise identical conditions; no absorption band was observed in the region around 2080 cm^{-1} (i.e., $<50 \mu\text{OD}$). In fact, in linear alkane solutions, the A_1 band absorption around 2080 cm^{-1} has not, to our knowledge, been observed experimentally. Experiments in cyclohexane, however, have reported the observation of a weak absorption at 2087 cm^{-1} .⁵¹ DFT calculations on hexane- and cyclohexane-solvated metal fragments indicate that the cyclohexane-solvated species has an absorption that is 3 times as intense as the hexane-solvated species. Thus, the calculated peak ratios and experimental observations are in excellent agreement with the alkyne solvation calculations.

B. Comparison of Group 6 Metal Coordination in Terminal Alkynes and Alcohols. The rearrangement of group 6 metal carbonyls in 1-hexanol is analogous to that of alkyne rearrangement and provides an ideal point of comparison. In the case of 1-hexanol, rearrangement occurs until the metal fragment coordinates to the hydroxyl group of the alcohol, at which point the rearrangement ceases.¹⁰ For $\text{Cr}(\text{CO})_6$ in room-temperature hexanol, the time scale for the rearrangement from an alkyl site to the final hydroxyl coordination is 1.2 ns, while the hexyne rearrangement is observed to occur on a time scale of 67 ps. Although this difference appears surprising at first glance, it is most likely due to differences in the viscosity of the two solvents. 1-Hexanol exhibits a viscosity of 6.00 cP,⁵² while 1-hexyne has a much lower viscosity of 0.34 cP.⁵³ According to the high friction limit of Kramers' theory,⁵⁴ the time constant of a reaction is proportional to a friction term that is related to the bulk viscosity via Einstein's diffusion relation and Stoke's law.⁵⁵ A more viscous solvent will result in a longer rearrangement time since the local solvent motions are smaller. The applicability of the bulk solvent viscosity in such a rearrangement process finds broad precedence in a variety of experiments.⁵⁶

C. Comparison of the Rearrangement Times for the Group 6 Metal Hexacarbonyls. While recent work has indicated that the process of rearrangement is an intermolecular process,^{10,57–63} there is no consensus on the details of the mechanism. Conventionally, rearrangement reactions of the type discussed here are described as associative, dissociative, or interchange.⁶⁴ Recent calculations by Harris and co-workers,⁶⁵ using the method of transition path sampling,^{66–69} have suggested that the mechanism responsible for such a rearrangement process can best be described as an interchange mechanism. Associative and dissociative mechanisms often used to describe rearrangement processes are the two extremes of an interchange mechanism. In the associative extreme, there is partial coordination of a surrounding solvent molecule followed by dissociation of the coordinated ligand. In this limit, rearrangement time scales for the three transition metal systems would be expected to correlate with the binding energies of the complex to alkynes in its more stable configuration (**2**). In the dissociative extreme, the coordinated ligand dissociates before a new species from the surrounding solvent can coordinate. The interchange mechanism is a hybrid of these two possibilities, where a solvent from the surrounding bath weakly interacts with the metal center at the same time as the coordinated ligand starts to dissociate.

While all three hexacarbonyl complexes, $\text{Cr}(\text{CO})_6$, $\text{Mo}(\text{CO})_6$, and $\text{W}(\text{CO})_6$, demonstrate the same rearrangement behavior, time constants for initial solvation and subsequent rearrangement from **1** to **2** differ. The time scales for the three metals and the mechanism of rearrangement can be understood in the context of the rearrangement mechanism by comparing the binding energies for each of the three metal complexes to alkyne in complexes **1** and **2**. The calculated bond dissociation energies for metal–alkyne interaction for the binding of acetylene to $\text{M}(\text{CO})_5$ [$\text{M} = \text{Cr}, \text{Mo}, \text{W}$] are shown in Table 6.⁷⁰ Also shown in Table 6 are the experimental binding energies of alkanes to $\text{M}(\text{CO})_5$ [$\text{M} = \text{Cr}, \text{Mo}, \text{W}$].⁷¹ $\text{W}(\text{CO})_5$ clearly forms the strongest bond with both the alkane and the alkyne and also coordinates on the

(48) Jiang, Y.; Lee, T.; Rose-Petruck, C. G. *J. Phys. Chem. A* **2003**, *107*, 7524.

(49) Fan, L.; Ziegler, T. *J. Phys. Chem.* **1992**, *96*, 6937.

(50) Jonas, V.; Thiel, W. *J. Chem. Phys.* **1995**, *102*, 8474.

(51) Paur-Afshari, R.; Lin, J.; Schultz, R. H. *Organometallics* **2000**, *19*, 1682.

(52) Dean, J. A. *Lange's Handbook of Chemistry*; McGraw-Hill Inc.: New York, 1999.

(53) Viswanath, D. S.; Natarajan, G. *Data Book on the Viscosity of Liquids*; Hemisphere Pub. Corp.: New York, 1989.

(54) Steinfeld, J. I.; Francisco, J. S.; Hase, W. L. *Chemical Kinetics and Dynamics*, 2 ed.; Prentice Hall: Upper Saddle River, NJ, 1998.

(55) Hansen, J. P.; McDonald, I. R. *Theory of Simple Liquids*, 2nd ed.; Academic Press: Orlando, 1986; p 206.

(56) Schroeder, J.; Troe, J. Solvent Effects in the Dynamics of Dissociation, Recombination, and Isomerization Reactions. In *Activated Barrier Crossing: Applications in Physics, Chemistry and Biology*; Fleming, G. R., Hanggigi, P., Eds.; World Scientific: Singapore, 1993; p 206.

(57) Breheny, C. J.; Kelly, J. M.; Long, C.; O'Keefe, S.; Pryce, M. T.; Russell, G.; Walsh, M. M. *Organometallics* **1998**, *17* (17), 3690.

(58) Creaven, B. S.; George, M. W.; Ginzburg, A. G.; Hughes, C.; Kelly, J. M.; Long, C.; McGrath, I. M.; Pryce, M. T. *Organometallics* **1993**, *12* (8), 3127.

(59) Krishnan, R.; Schultz, R. H. *Organometallics* **2001**, *20* (15), 3314.

(60) Ladogana, S.; Nayak, S. K.; Smit, J. P.; Dobson, G. R. *Organometallics* **1997**, *16* (13), 3051.

(61) Ladogana, S.; Nayak, S. K.; Smit, J. P.; Dobson, G. R. *Inorg. Chem.* **1997**, *36*, 650.

(62) Lugovskoy, S.; Lin, J.; Schultz, R. H. *Dalton Trans.* **2003** (15), 3103.

(63) Lugovskoy, A.; Shagal, A.; Lugovskoy, S.; Huppert, I.; Schultz, R. H. *Organometallics* **2003**, *22* (11), 2273.

(64) Cotton, F. A.; Wilkenson, G.; Gauss, P. L. *Basic Inorganic Chemistry*; John Wiley and Sons: Toronto, 1995.

(65) Snee, P. T.; Shanoski, J. E.; Harris, C. B. *J. Am. Chem. Soc.* **2005**, *127*, 1286.

(66) Dellago, C.; Bolhuis, P. G.; Chandler, D. *J. Chem. Phys.* **1998**, *108*, 9236.

(67) Dellago, C.; Bolhuis, P. G.; Csajka, F. S.; Chandler, D. *J. Chem. Phys.* **1998**, *108*, 1964.

(68) Dellago, C.; Bolhuis, P. G.; Chandler, D. *J. Chem. Phys.* **1999**, *110*, 6617.

(69) Geissler, P. L.; Chandler, D. *J. Chem. Phys.* **2000**, *113*, 9759.

(70) Nechaev, M. S.; Rayon, V. M.; Frenking, G. *J. Phys. Chem. A* **2004**, *108*, 3134.

(71) Morse, J. M., Jr.; Parker, G. H.; Burkey, T. J. *Organometallics* **1989**, *8*, 2471.

Table 6. Binding Energy of M(CO)₅ to Acetylene^a and Heptane^b (in kcal/mol)

	Cr(CO) ₅	Mo(CO) ₅	W(CO) ₅
L = C ₂ H ₂	19.6	18.0	25.3
L = C ₇ H ₁₄	9.6 ± 2.3	8.7 ± 2.7	13.4 ± 2.8

^a Theoretical calculations from ref 70. ^b Experimental data from ref 71.

fastest time scale; Mo(CO)₅ and Cr(CO)₅ have binding energies that are much weaker and coordinate on longer time scales. There is an anticorrelation between the bond strength and the rearrangement time. This behavior is indicative of an associative mechanism, where the rate constant for rearrangement from species **1** to species **2** is expected to be proportional to the binding energies. A purely dissociative mechanism can be directly ruled out since the metal with the weakest interaction with the alkane in structure **1** would be expected to dissociate most readily. Rearrangement would then occur on the fastest time scale for the weakest interaction, in direct contrast with the time constants measured for this rearrangement process. A mechanism with mainly associative character is in agreement with the experimental data. However, as suggested by our recent work, a dissociative interchange mechanism may be the best description of this process.

D. Tautomerization of the π -Bonded Complex to the Vinylidene Metal Complex. According to earlier proposed mechanisms for the photoinduced chemistry of metal hexacarbonyls in alkynes, triple-bond coordinated alkyne complexes **2** eventually tautomerize to the corresponding vinylidene complex **3**. According to the spectral evidence provided by our experiments, the formation of a vinylidene complex does not occur on the ultrafast time scale. Previous work in low-temperature matrixes assigns two peaks to the vinylidene species. For the tungsten carbonyl complex these peaks are at 2002 and 2079 cm⁻¹ and correspond to the E and A₁ bands of the complex. Due to possible spectral overlap with the triple-bond coordinated complex, the peak at 2079 cm⁻¹ cannot be used in our studies to directly indicate whether the tautomerization to a vinylidene complex occurs on the ultrafast time scale. The intensity of this absorption, however, is expected to be at least 5 times more intense than the corresponding absorption of **2** according to DFT calculations and previous experiments.^{6,12,13} No increase in this absorption is observed after the measured rearrangement time. Further, the peak at 2002 cm⁻¹ is a peak of substantial intensity (comparable to the A₁ peak at 1929 cm⁻¹ in **1**) that should be easily discernible in our time-resolved IR experiments if present. None of the three metals studied in the present work display such a feature. Finally, if a rearrangement of **2** to **3** were occurring, the kinetic traces for the A₁ and E band on the red side (lower energy) of the bleach should decay; no decay is observed. The lack of a strong absorption at 2080 or 2002 cm⁻¹ and any observable kinetic changes in the other absorption frequencies of **2** lead to the conclusion that tautomerization to the vinylidene species does not occur under the conditions of these experiments on the time scales that we have investigated.

Preliminary studies were carried out using a step- and rapid-scan FTIR instrument, described elsewhere,⁷² to investigate the rearrangement behavior of the triple-bond coordinated complex on the nanosecond to millisecond time scale. The presence of a vinylidene complex was not observed in the spectra collected. The same spectral features present in the ultrafast data are observed in the long-time data without change. In fact, these experiments show no dynamical behavior. The experimental observation that no vinylidene complex forms on the millisecond time scale indicates that the free energy barrier to this tautomerization is at least 13 kcal/mol. DFT calculations done by De Angelis and co-workers¹⁶ for M(CO)₅-HC≡CCH₃ (M = Cr, Mo, W) indicate that the *highest* transition states in the *lowest* energy pathway for the tautomerization from **2** to **3** exhibit barriers of 21.7 (W), 22.6 (Cr), and 23.3 kcal/mol (Mo). Furthermore, the reaction is found to be slightly endothermic with 2.4, 5.2, and 6.9 kcal/mol for W, Cr, and Mo, respectively (reaction enthalpies including zero-point and thermal energy corrections for 298 K), thus favoring an alkyne coordination (**2**) over vinylidene coordination (**3**) for the transition metal complexes studied here.

Our findings conflict with earlier observations in low-temperature matrix studies.¹¹ Thermal tautomerization from **2** to **3** is expected to be negligible at low temperatures, yet matrix experiments indicate high yields of **3**. A sequential photon mechanism in which **3** is formed from **2** via the absorption of an additional photon may explain such an observation as was originally presented in matrix studies.^{12,13} Such a mechanism would not be seen in the ultrafast experiments described here since the applied pulses of light are too short as compared with the formation time of **2**. In contrast, continuous irradiation of the sample may result in formation of the vinylidene species and explain the high yields observed in the matrix studies.

IV. Conclusions

We have investigated the mechanism of coordination of terminal alkynes to metal carbonyl complexes of the type M(CO)₆ (M = Cr, Mo, W). The initial steps in the solvation of a coordinatively unsaturated metal center are consistent with previous studies of linear alcohols and silanes. In unsaturated hydrocarbons, this process involves the initial coordination of a neighboring solvent molecule followed by rearrangement to a more stable, π -coordinated complex. On the basis of experimentally measured rates of rearrangement and calculated binding energies, a dissociative mechanism can be ruled out in favor of an associative or dissociative interchange mechanism for the rearrangement of terminal alkynes coordinating to transition metal complexes. In these experiments, tungsten forms the strongest bond to the alkyne and was found to rearrange on the fastest time scale.

The tautomerization of a π -bonded complex to its vinylidene analogue was not observed on the femtosecond through millisecond time scale, indicating a significant barrier to the tautomerization. These results were verified using DFT calculations. Current experi-

ments are aimed at investigating the possibility of a sequential photon process for the tautomerization from an alkyne to a vinylidene-coordinated species.

Acknowledgment. We thank the National Science Foundation for funding, and the Office of Basic Energy Sciences, Chemical Sciences Division, of the U.S. Department of Energy under contract DE-AC03-76SF0-00098 for the use of some specialized equipment. M.F.K. acknowledges support by the Alexander von Humboldt foundation through a Feodor-Lynen Fellowship. The

authors would like to thank H. Frei for the use of the step- and rapid-scan FTIR spectrometer and helpful discussions.

Supporting Information Available: Ultrafast spectra for $\text{Mo}(\text{CO})_6$ and $\text{W}(\text{CO})_6$ and the step-scan spectrum for $\text{Mo}(\text{CO})_6$ in 1-hexyne are provided. Coordinates for optimized structures and full frequency analysis for all three complexes of Cr are provided. This information is available free of charge via the Internet at <http://pubs.acs.org>.

OM049101M